

# Scalarized Hairy Black Holes

Burkhard Kleihaus<sup>a</sup>, Jutta Kunz<sup>a</sup> and Stoytcho Yazadjiev<sup>b</sup>

<sup>a</sup>Institut für Physik, Universität Oldenburg, Postfach 2503  
D-26111 Oldenburg, Germany

<sup>b</sup>Department of Theoretical Physics, Faculty of Physics, Sofia University  
Sofia 1164, Bulgaria

August 27, 2018

## Abstract

In the presence of a complex scalar field scalar-tensor theory allows for scalarized rotating hairy black holes. We exhibit the domain of existence for these scalarized black holes, which is bounded by scalarized rotating boson stars and ordinary hairy black holes. We discuss the global properties of these solutions. Like their counterparts in general relativity, their angular momentum may exceed the Kerr bound, and their ergosurfaces may consist of a sphere and a ring, i.e., form an ergo-Saturn.

## 1 Introduction

One of the major discoveries in physics during the last two decades was the accelerated expansion of the Universe. General relativity and the standard model of particle physics fail to explain this phenomenon. This situation calls for new alternative ideas able to give a satisfactory explanation of the cosmological observations. One of the possibilities is to go beyond general relativity and to consider more general theories of gravity.

Among the most natural generalizations of the original Einstein theory are the scalar-tensor theories [1, 2, 3, 4, 5].

These theories are viable gravitational theories and can pass all known experimental and observational constraints. In addition, they can explain the accelerated expansion of the Universe. The scalar-tensor generalizations of the original Einstein theory naturally arise in the context of the modern unifying theories as string theory and Kaluza-Klein theories.

In scalar-tensor theories the gravitational interaction is mediated not only by the spacetime metric but also by an additional scalar field. From a physical point of view this scalar field plays the role of a variable gravitational constant.

General relativity (GR) is well-tested in the weak-field regime, whereas the strong-field regime remains largely unexplored and unconstrained. In the strong-field regime one expects the differences between GR and alternative theories of gravity to be more pronounced. The natural laboratories for testing the strong-field regime of gravitational theories are compact stars and black holes.

There exist scalar-tensor theories which are indistinguishable from GR in the weak-field regime but which can differ significantly from GR in the strong-field regime. An example of such a phenomenon is the so-called spontaneous scalarization, observed in a certain class of scalar-tensor theories. When spontaneous scalarization takes place, in addition to the general relativistic solutions with a trivial scalar field, there exist further solutions with a nontrivial scalar field. In fact, these scalarized solutions are energetically more favorable than their GR counterparts.

Spontaneous scalarization was first observed for neutron stars [6], where *spectacular changes* were seen in static equilibrium configurations for a given nuclear equation of state. More recently, spontaneous scalarization was also observed in rapidly rotating neutron stars [7, 8], where the deviations of the rapidly rotating scalar-tensor neutron stars from the general-relativistic solutions were even significantly larger than in the static case.

Spontaneous scalarization was also observed for static uncharged and charged boson stars [9, 10, 11]. The first purpose of the present paper is to study rapidly rotating boson stars in scalar-tensor theories, and to establish the phenomenon of spontaneous scalarization for these stationary compact objects. The second purpose of this paper is to address the existence of scalarized hairy black holes.

In General Relativity (GR) rotating vacuum black holes are described in terms of the Kerr solution. This solution specifies the full spacetime in terms of only two parameters, its mass and its angular momentum. Hairy black holes appear, when suitable matter fields are included. Examples are chiral fields, Yang-Mills and Higgs fields, yielding hairy static black holes [12, 13, 14, 15] as well as rapidly rotating hairy black holes [16, 17].

Recently it was noted, that also a single complex scalar field allows for hairy black holes, provided the black holes are rotating [18]. In fact, these solutions may be viewed as a generalization of rotating boson stars, that are endowed with a horizon. The regular boson stars form part of the boundary of the domain of existence of this new type of hairy black holes. The other parts of the boundary exist of extremal hairy black holes and scalar clouds.

Here we show, that besides these rapidly rotating hairy black holes, already present in GR, scalar-tensor theory again allows for the phenomenon of scalarization. In particular, we study the physical properties of these scalarized hairy black holes, and map their domain of existence.

## 2 Scalar-Tensor Theories

Denoting the gravitational scalar by  $\Phi$ , the gravitational action of scalar-tensor theories in the physical Jordan frame is given by

$$S = \frac{1}{16\pi G_*} \int d^4x \sqrt{-\tilde{g}} \left( F(\Phi) \tilde{R} - Z(\Phi) \tilde{g}^{\mu\nu} \partial_\mu \Phi \partial_\nu \Phi - 2W(\Phi) \right) + S_m[\Psi_m; \tilde{g}_{\mu\nu}], \quad (1)$$

where  $G_*$  is the bare gravitational constant,  $\tilde{g}_{\mu\nu}$  is the spacetime metric,  $\tilde{R}$  is the Ricci scalar curvature, and  $S_m[\Psi_m; \tilde{g}_{\mu\nu}]$  denotes the action of the matter fields.

The functions  $F(\Phi)$ ,  $Z(\Phi)$  and  $W(\Phi)$  are subject to physical restrictions: We require  $F(\Phi) > 0$ , since gravitons should carry positive energy, and  $2F(\Phi)Z(\Phi) + 3[dF(\Phi)/d\Phi]^2 \geq 0$ , since the kinetic energy of the scalar field should not be negative. The matter action  $S_m$  depends on the matter field  $\Psi_m$  and on the space-time metric  $\tilde{g}_{\mu\nu}$ . The matter action does not involve the gravitational scalar field  $\Phi$  in order to satisfy the weak equivalence principle.

Variation of the action with respect to the spacetime metric and the gravitational scalar as well as the matter field leads to the field equations in the Jordan frame. However, these field equations are rather involved. It is therefore easier to consider a mathematically equivalent formulation of scalar-tensor theories in the conformally related Einstein frame with metric  $g_{\mu\nu}$

$$g_{\mu\nu} = F(\Phi) \tilde{g}_{\mu\nu}. \quad (2)$$

In the Einstein frame the action then becomes (up to a boundary term)

$$S = \frac{1}{16\pi G_*} \int d^4x \sqrt{-g} \left( R - 2g^{\mu\nu} \partial_\mu \varphi \partial_\nu \varphi - 4V(\varphi) \right) + S_m[\Psi_m; \mathcal{A}^2(\varphi) g_{\mu\nu}], \quad (3)$$

where  $R$  is the Ricci scalar curvature with respect to the Einstein metric  $g_{\mu\nu}$ ,  $\varphi$  represents the new scalar field defined via

$$\left( \frac{d\varphi}{d\Phi} \right)^2 = \frac{3}{4} \left( \frac{d \ln(F(\Phi))}{d\Phi} \right)^2 + \frac{Z(\Phi)}{2F(\Phi)} \quad (4)$$

with the new functions

$$\mathcal{A}(\varphi) = F^{-1/2}(\Phi) , 2V(\varphi) = W(\Phi)F^{-2}(\Phi).$$

By varying this action with respect to the metric in the Einstein frame  $g_{\mu\nu}$ , the scalar field  $\varphi$ , and the matter field  $\Psi_m$ , we find the set of field equations in the Einstein frame.

In particular, we here consider a scalar tensor theory with potential  $V(\varphi) = 0$  and function  $\mathcal{A}(\varphi)$  [6]

$$\ln \mathcal{A}(\varphi) = \frac{1}{2}\beta\varphi^2 . \quad (5)$$

We present a systematic study for the parameter value  $\beta = -4.7$ , but we have also done calculations for larger values of  $\beta$ .

For the matter action we choose a complex boson field  $\Psi$

$$S_m[\Psi_m; \tilde{g}_{\mu\nu}] = - \int d^4x \sqrt{-g} \left[ \frac{1}{2} \mathcal{A}^2(\varphi) g^{\mu\nu} (\Psi_{,\mu}^* \Psi_{,\nu} + \Psi_{,\nu}^* \Psi_{,\mu}) + \mathcal{A}^4(\varphi) U(|\Psi|) \right] \quad (6)$$

with self-interaction potential

$$U(|\Psi|) = m_b^2 |\Psi|^2 + \Lambda |\Psi|^4 . \quad (7)$$

### 3 Properties

To obtain stationary hairy black hole and boson star solutions we employ the line element

$$ds^2 = -f_0 N dt^2 + \frac{f_1}{f_0} \left( f_2 \left[ \frac{1}{N} d\bar{r}^2 + \bar{r}^2 d\theta^2 \right] + \bar{r}^2 \sin^2 \theta [d\varphi - f_3 dt]^2 \right) , \quad (8)$$

with the metric functions  $f_i(\bar{r}, \theta)$ ,  $i = 0, \dots, 3$ , and

$$N = 1 - \frac{\bar{r}_H}{\bar{r}} ,$$

where  $\bar{r}_H$  denotes the horizon parameter. For the boson stars we set  $\bar{r}_H = 0$ , i.e.  $N = 1$ . Likewise, we parametrize the gravitational scalar field  $\Phi$  by  $\Phi(\bar{r}, \theta)$ .

For the boson field  $\Psi$  we adopt the stationary Ansatz

$$\Psi = \psi(\bar{r}, \theta) e^{i\omega t + in\phi} \quad (9)$$

where  $\psi$  is a real function,  $\omega$  denotes the boson frequency, and  $n$  – as required by the single-valuedness of the scalar field – is an integer representing a rotational quantum number.

In the Lagrangian for the boson field  $\Psi$  we employ a quartic self-interaction potential (7) with coupling constant  $\Lambda$ . While we present our results for the value  $\Lambda = 300$ , we have also performed calculations for other values of  $\Lambda$ .

As in [18] we introduce a new radial coordinate

$$r = \sqrt{\bar{r}^2 - \bar{r}_H^2} \quad (10)$$

such that  $0 \leq r < \infty$ , and the event horizon is located at  $r = 0$ . The functions satisfy the following set of boundary conditions, obtained from the requirements of asymptotic flatness as well as of regularity at the origin and the event horizon in the case of the boson star, resp. black hole solutions

$$\partial_r f_i(0, \theta) = 0, \quad i = 0, 1, 2, \quad \psi(0, \theta) = 0, \quad \partial_r \phi(0, \theta) = 0 \quad (11)$$

$$f_i(\infty, \theta) = 1, \quad i = 0, 1, 2, \quad f_3(\infty, \theta) = 0, \quad \psi(\infty, \theta) = \phi(\infty, \theta) = 0 \quad (12)$$

$$\partial_\theta f_i(r, 0) = 0, \quad i = 0, 1, 3, \quad f_2(r, 0) = 1, \quad \psi(r, 0) = 0, \quad \partial_\theta \phi(r, 0) = 0 \quad (13)$$

$$\partial_\theta f_i(r, \pi/2) = 0, \quad i = 0, 1, 2, 3, \quad \partial_\theta \psi(r, \pi/2) = \partial_\theta \phi(r, \pi/2) = 0, \quad (14)$$

and  $\partial_r f_3(0, \theta) = 0$ , resp.  $f_3(0, \theta) = \Omega_H$  for boson star and black hole solutions.

The mass  $M$  and the angular momentum  $J$  of stationary asymptotically flat space-times can be obtained in scalar-tensor theory - analogously to GR - from the asymptotic behavior of the metric functions  $f_0$  and  $f_3$ , respectively,

$$f_0 \rightarrow 1 - 2\mu/r, \quad f_3 \rightarrow 2J/r^3, \quad (15)$$

and

$$M = \mu + \frac{\bar{r}_H}{2}. \quad (16)$$

Since the action is invariant under the global phase transformation  $\Psi \rightarrow \Psi e^{i\chi}$ , a conserved current arises

$$j^\mu = -i\mathcal{A}^2(\varphi) (\Psi^* \partial^\mu \Psi - \Psi \partial^\mu \Psi^*), \quad j^\mu_{;\mu} = 0. \quad (17)$$

It is associated with the Noether charge  $Q$  representing the particle number,

$$Q = \int_\Sigma \sqrt{-g} j^0 d\bar{r} d\theta d\varphi \quad (18)$$

At the event horizon of the hairy black holes the Killing vector  $\chi$

$$\chi = \xi + \Omega_H \eta \quad (19)$$

is null, and  $\Omega_H$  represents the horizon angular velocity. Hairy black holes satisfy [18]

$$\omega = n\Omega_H \quad (20)$$

We denote the horizon area by  $A_H$  in the Einstein frame, and define the areal horizon radius by

$$R_H = \sqrt{A_H/4\pi}. \quad (21)$$

The horizon temperature by  $T_H$  is obtained from the surface gravity  $\kappa_{\text{sg}}$ ,

$$\kappa_{\text{sg}}^2 = -\frac{1}{2} (\nabla_\mu \chi_\nu) (\nabla^\mu \chi^\nu) \Big|_H, \quad (22)$$

and  $T = \kappa_{\text{sg}}/2\pi$ .

We note, that the limit  $\bar{r}_H \rightarrow 0$  comprises two different types of configurations<sup>1</sup>:

- (i) Extremal black holes are obtained, when  $T_H \rightarrow 0$ ,
- (ii) Globally regular solutions are obtained, when  $A_H \rightarrow 0$ .

The latter correspond to rotating boson stars. For boson stars  $J = nQ$ .

## 4 Results

We have obtained rapidly rotating scalarized boson stars and hairy black hole solutions for a sequence of rotational quantum numbers  $n > 0$ . To this end we have solved the set of coupled non-linear partial differential equations subject to the appropriate boundary conditions with a numerical algorithm based on the Newton-Raphson method [22]. Compactifying space by introducing the radial coordinate

$$x = \frac{r}{1+r}. \quad (23)$$

we have discretized the equations on a non-equidistant grid in  $x$  and  $\theta$ , with typical grid sizes on the order of  $250 \times 65$ , covering the integration region  $0 \leq x \leq 1$  and  $0 \leq \theta \leq \pi/2$ . In the following we will use scaled quantities  $M/M_0$ ,  $Q/Q_0$ ,  $\omega/\omega_0$ ,  $J/J_0$ , and  $R_H/r_0$ , with  $M_0 = m_{\text{Pl}}^2/m_b$ ,  $Q_0 = J_0 = m_{\text{Pl}}^2/m_b^2$ ,  $\omega_0 = m_b$ ,  $r_0 = 1/m_b$ , where  $m_{\text{Pl}}$  denotes the Plack mass.

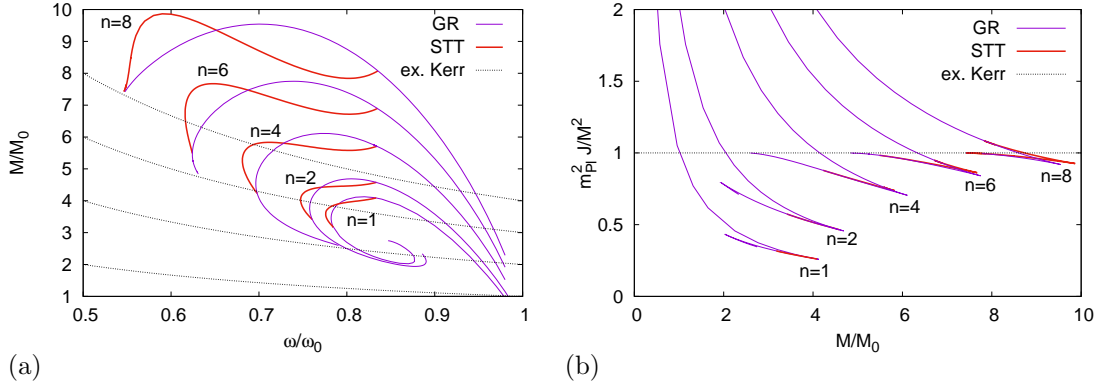


Figure 1: Families of scalarized (thick red) and ordinary (thin blue) boson star solutions for rotational quantum number  $n = 1, 2, 4, 6$  and  $8$  as well as the corresponding curve(s) for the extremal Kerr solution (dotted black). (a) The scaled mass  $M/M_0$  versus the scaled boson frequency  $\omega/\omega_0$ . (For black holes  $\omega = n\Omega_H$ .) (b) The scaled angular momentum  $m_{p1}^2 J/M^2$  versus the scaled mass  $M/M_0$ .

#### 4.1 Scalarized boson stars

The globally regular ordinary boson star solutions form a large part of the boundary of the domain of existence of the hairy black hole solutions [18]. Let us therefore first consider the boson star solutions. In Fig. 1(a) the scaled mass  $M/M_0$  of the boson star solutions is exhibited versus the scaled boson frequency  $\omega/\omega_0$  for rotational quantum numbers  $n = 1, 2, 4, 6$  and  $8$ . The families of ordinary boson star solutions emerge from the vacuum at  $\omega = m_b = \omega_0$ . They form a first (and at least in part classically stable) branch, until the mass reaches its maximal value. We note, that this maximal value of the mass increases rapidly with  $n$ .

Beyond the maximal mass the families of ordinary boson star solutions continue in a spiral-like manner for the lowest values of  $n$ . They end in a merger solution, where a branch of extremal hairy black hole solutions is encountered [18]. For the higher  $n$ , however, they feature only a single further branch, their second branch, before they merge with a branch of extremal hairy black hole solutions. Interestingly, each of these higher  $n$  second branches of boson star solutions ends close to an extremal Kerr black hole solution, possessing almost the same mass and the respective horizon angular velocity  $\Omega_H = \omega/n$ .

When considering the scaled angular momentum  $m_{p1}^2 J/M^2$  of these ordinary boson star solutions versus the mass  $M/M_0$  as exhibited in Fig. 1(b) together with the line  $m_{p1}^2 J/M^2 = 1$  of extremal Kerr black holes, the branches form cusps at extremal values of the mass. The lower  $n$  solutions therefore feature several cusps, whereas the higher  $n$  solutions have a single cusp. Clearly, for the higher  $n$  families of boson star solutions the second branches approach the extremal Kerr value closely, when they end in a merger solution, where a branch of extremal hairy black hole solutions is encountered.

In addition, Fig. 1 exhibits the scalarized boson star solutions associated with the ordinary boson star solutions. For a given value of  $n$  the scalarization arises at a critical value of the boson frequency,  $\omega_{cr}^1$ , where a branch of scalarized boson star solutions emerges from the first branch of ordinary boson star solutions. Interestingly,  $\omega_{cr}^1$  is rather independent of the rotational quantum number  $n$ . The families of scalarized boson stars then extend up to a second critical value  $\omega_{cr}^2$ , where they merge again into the respective second branch of ordinary boson stars. Since  $\omega_{cr}^2$  decreases with  $n$ , the domain of existence of rapidly rotating scalarized boson stars increases with  $n$ .

For  $n = 1$ , the critical point  $\omega_{cr}^1$  is close to but slightly below the maximal value of the mass of the ordinary boson stars. Since the mass of the scalarized boson stars decreases monotonically until the critical point  $\omega_{cr}^2$  is reached, and since the same holds for the particle number  $Q$ , the

<sup>1</sup>Recall, that an extremal black hole has a vanishing horizon parameter in the coordinates employed.

ordinary boson stars are stable with respect to scalarization along their first branch. Indeed, for a given value of  $Q$  along their first branch the mass of the ordinary boson stars is always lower than the mass of the scalarized boson stars, when these exist. For  $n = 2$  the situation is analogous.

For  $n \geq 3$ , however, the scalarized boson stars assume their maximal mass no longer at  $\omega_{\text{cr}}^1$ , but at a smaller value of  $\omega$ . Thus they form a (potentially) stable branch, starting at the first minimum of the mass and extending until their global maximum. Along this branch, the scalarized boson stars represent the energetically favored solutions. Thus ordinary boson stars will be unstable with respect to scalarization in this range of frequencies.

We note, that the maximal mass of the scalarized boson stars increases with  $n$ . However, unlike the case of rapidly rotating neutron stars, where the maximal mass reached for scalarized neutron stars significantly exceeds the maximal mass of ordinary neutron stars, the maximal mass of scalarized boson stars does not deviate too strongly from the one of ordinary boson stars.

Considering the end point of the families of scalarized boson star solutions, we note that for the larger values of  $n$ , with increasing  $n$  the end point gets closer to the end point of the respective family of ordinary boson star solutions. In particular, the second branches of the ordinary boson star solutions shorten with increasing  $n$ . For  $n = 8$ , the end points of both ordinary and scalarized boson star solutions are rather close to each other.

## 4.2 Scalarized hairy black holes

Let us now turn to the hairy black holes. Starting from a generic ordinary boson star solution, a sequence of hairy black holes emerges, when the presence of a small horizon is imposed, and the horizon is then increased in size. The domain of existence of hairy black holes is then mapped by varying the horizon size and the horizon angular velocity.

For ordinary hairy black holes, the domain of existence has been studied before for  $n = 1$  and 2 [18], employing only a mass term for the boson field. There it was shown, that the boundary of the domain of existence of these solutions consists of

- (i) the family of boson stars, and the associated families of
- (ii) extremal hairy black holes and
- (iii) scalar clouds [19, 20].

We exhibit in Fig. 2 the domain of existence of ordinary hairy black holes for the case of the  $\Phi^4$  potential, and rotational quantum numbers  $n = 1, 4$  and 8. In particular, we here show the scaled mass  $M/M_0$  (left column) and the scaled particle number  $Q/Q_0$  (right column) of the hairy black holes versus the scaled boson frequency  $\omega/\omega_0$ . We note, that for black holes  $\omega = n\Omega_H$ . Here we have included the case  $n = 1$ , to allow for direct comparison with the case without self-interaction [18]. Studies of the rotational quantum numbers  $n > 3$  were not reported before, neither with nor without self-interaction. In all these figures, the beige regions labelled GR represent the domain of existence of the ordinary hairy black holes.

The families of extremal hairy black hole solutions possess two endpoints. At one endpoint they join the respective branch of globally regular boson stars solutions in a merger solution. At the other endpoint they join precisely the respective branch of scalar cloud solutions. These latter endpoints are marked in the figures by an asterisk.

In these figures the sets of extremal hairy black hole solutions have been obtained by extrapolation, where the horizon parameter  $\bar{r}_H$  was decreased towards zero.<sup>2</sup> The hair of these extremal black hole solutions becomes evident, for instance, when inspecting the scaled particle number  $Q/Q_0$  of these extremal solutions:  $Q$  is always finite (see Fig. 2).

As seen in Fig. 2 for  $n = 1$ , the extremal hairy black hole solutions still form part of a spiral, whereas for the higher values of  $n$  this spiralling pattern is lost. For  $n = 4$  and in particular for  $n = 8$ , the mass of the extremal hairy black hole solutions is close to the mass of the extremal Kerr black holes. The particle number of these extremal hairy black holes is, however, clearly

---

<sup>2</sup>We note, that the extrapolation is no longer completely reliable in the innermost region of the spiral-like part for the  $n = 1$  case.

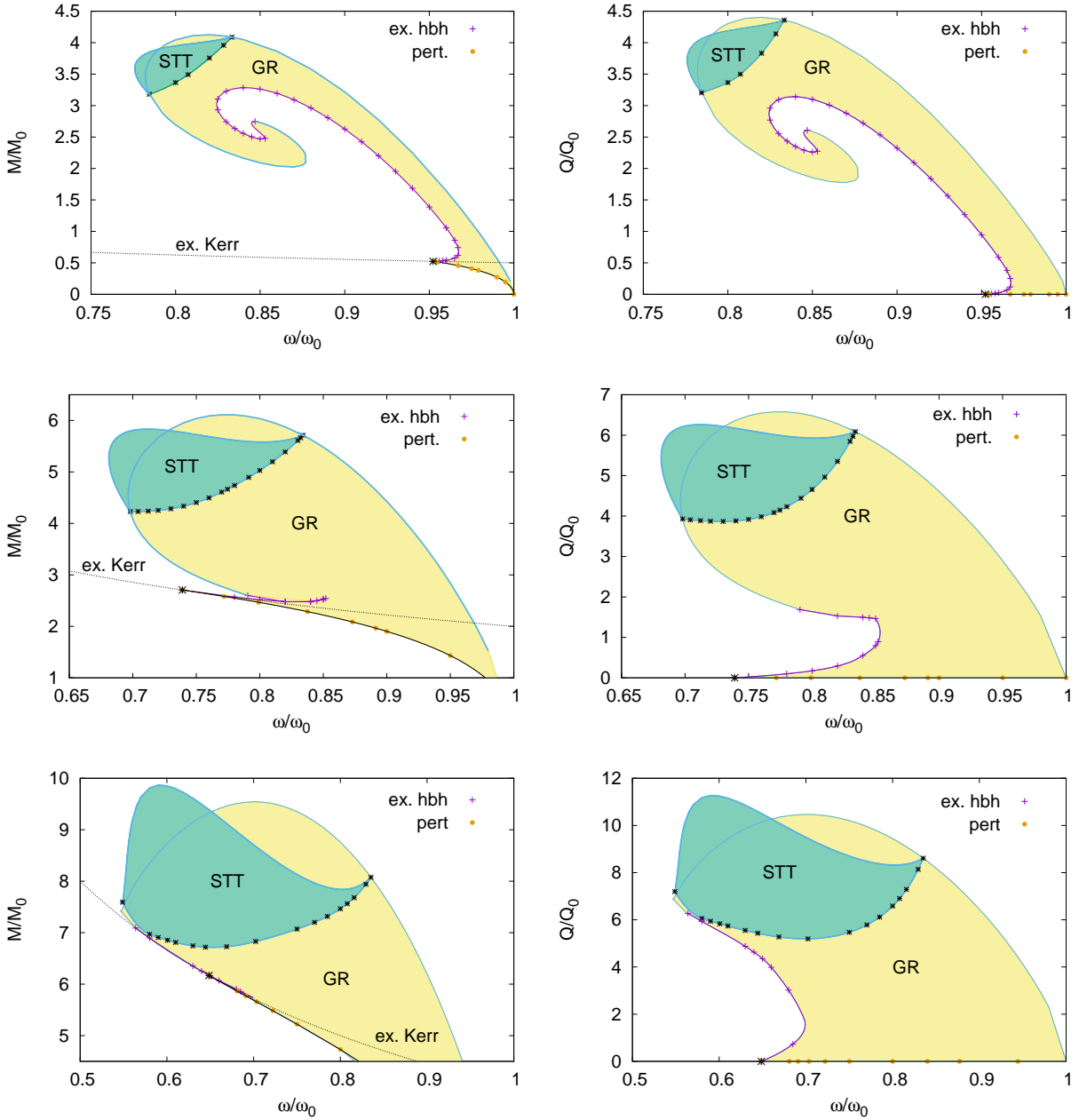


Figure 2: Domains of existence of scalarized (green) and ordinary (beige) hairy black hole solutions for rotational quantum numbers  $n = 1$  (upper),  $n = 4$  (middle) and  $n = 8$  (lower). Shown are the scaled mass  $M/M_0$  (left column) and the scaled particle number  $Q/Q_0$  (right column) versus the scaled boson frequency  $\omega/\omega_0$ . (For black holes  $\omega = n\Omega_H$ .) The boundaries are formed by boson star solutions, extremal hairy black hole solutions, and perturbative scalar clouds. The mass of extremal Kerr solutions is also shown.

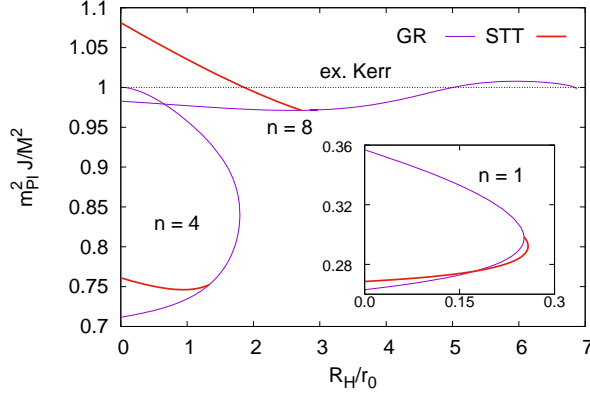


Figure 3: The scaled angular momentum  $m_{P1}^2 J/M^2$  is shown versus the scaled areal horizon radius  $R_H/r_0$  (21) for a fixed value of the boson frequency,  $\omega/\omega_0 = 0.8$  for hairy black holes in GR (thin blue) and scalarized hairy black holes (STT) (thick red). Also shown is the Kerr bound,  $m_{P1}^2 J/M^2 = 1$ .

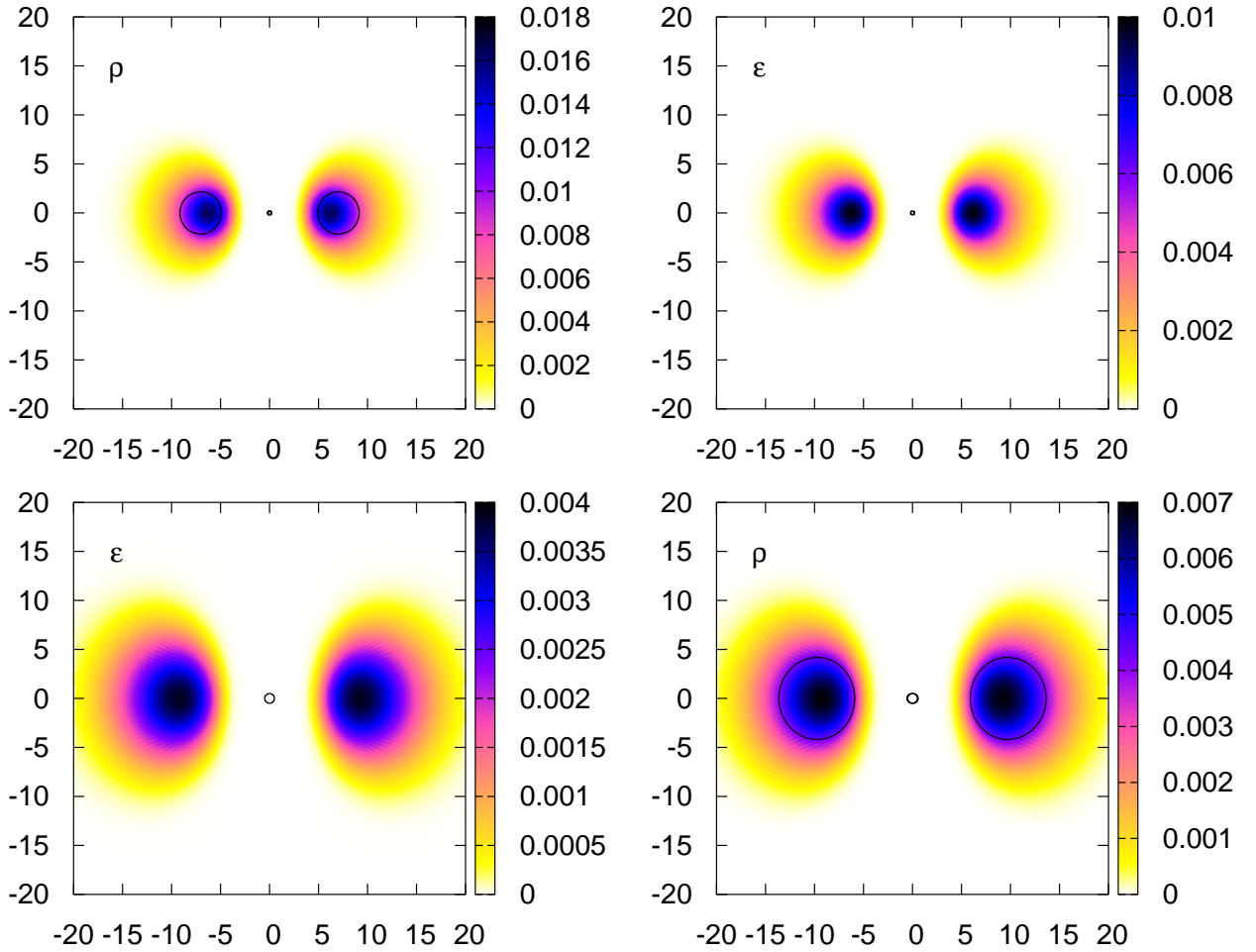


Figure 4: Contour plots of the energy-momentum tensor component  $\varepsilon = -T_0^0$  (left column) and the particle number density  $\rho = j^0$  (right column) for hairy black holes with rotational quantum number  $n = 8$ , boson frequency  $\omega = 0.65\omega_0$ , and mass  $M = 9M_0$  in GR (top) and with scalarization (STT) (bottom). The axes are  $\bar{y} = \pm\bar{r}\sin\theta$  and  $\bar{z} = \bar{r}\cos\theta$ , both in units of  $r_0$ . The solid circles mark the horizon, the dashed lines the ergosurface.



finite and reaches zero only when the scalar cloud solutions are reached. The study of  $Q$  therefore helps to clarify the domain of existence and its boundaries.

Let us now consider the domain of existence of the scalarized hairy black holes. It is also exhibited in Fig. 2 and marked by the green region labelled STT. The upper boundary of this domain of existence is always given by the regular scalarized boson stars. The lower boundary is reached somewhere within the domain of existence of ordinary hairy black holes, at the moment that the scalarization disappears. Thus we do not observe extremal scalarized hairy black holes.

There is always a part of the domain of existence of scalarized hairy black holes, where there are no ordinary hairy black holes. This part increases with increasing  $n$ . For the lower  $n$ , scalarized black holes exist for smaller boson frequencies, for the higher  $n$  scalarized hairy black holes reach higher values of the mass and the particle number than ordinary hairy black holes.

Kerr black holes satisfy the bound  $m_{\text{P}1}^2 J/M^2 \leq 1$ . But this bound may be exceeded by hairy black holes [18, 21]. We demonstrate this in Fig. 3 for several families of hairy black holes. In particular, we exhibit the scaled angular momentum  $m_{\text{P}1}^2 J/M^2$  versus the areal horizon radius  $R_{\text{H}}/r_0$  (21) for hairy black holes with  $\omega/\omega_0 = 0.8$ ,  $n = 4$  and  $n = 8$  in GR and with scalarization (STT). We note, that scalarized hairy black holes can also exceed the Kerr bound.

We exhibit in Fig. 4 contour plots of the component  $\varepsilon = -T_0^0$  of the energy momentum tensor (left column) and of the particle number density  $\rho = j^0$  (right column) of a hairy black hole in GR (top) and a scalarized hairy black hole (bottom). For comparison, we have chosen the same rotational quantum number  $n = 8$ , boson frequency  $\omega = 0.65\omega_0$  and mass  $M = 9M_0$  for these black holes.

The central black hole in GR has a horizon area of  $A_{\text{H}} \approx 0.79r_0^2$  and is thus much smaller than the scalarized black hole with  $A_{\text{H}} \approx 3r_0^2$ . Both  $\varepsilon$  and  $\rho$  are concentrated in tori around the central black hole. The maximal value of  $\varepsilon$  is considerably larger for the GR black hole than for the scalarized one, while the maximal value of  $\rho$  is only slightly larger.

In the figures showing  $\rho$  also the ergosurfaces are indicated. Ordinary hairy black holes can feature ergosurfaces consisting of an ergosphere and an ergoring, forming together an ergo-Saturn [18]. This is also the case for the GR black hole shown. Here we note, that the same phenomenon may hold as well for scalarized hairy black holes. Their ergosurface may also represent an ergo-Saturn, as depicted in the figure.

## 5 Conclusions

Scalar-tensor theories of gravity offer several observable consequences (see e.g., [23] and references therein). Here we have concentrated on the effect scalarization. First, we have shown that scalarization occurs for rapidly rotating boson stars (with a fourth order self-interaction).

Rotating boson stars possess a rotational quantum number, an integer  $n$ . Constructing families of boson stars for  $n = 1, \dots, 8$ , we have shown, that with increasing  $n$ , the scalarization becomes more pronounced. We expect this trend to continue.

Subsequently, we have constructed hairy black holes. After mapping out the domain of existence of hairy black holes in GR, which is bounded by boson stars, extremal hairy black holes and scalar clouds, we have surveyed the domain of existence of scalarized black holes. One boundary of their domain of existence is formed by scalarized boson stars. The other boundary, however, is formed by ordinary hairy black holes. Here the scalar field simply vanishes, thus reducing the solutions to general relativistic solutions with a trivial scalar field.

We have shown that the physical properties of the scalarized hairy black holes resemble in many respects those of hairy black holes in GR. For instance, they may substantially exceed the Kerr bound  $m_{\text{P}1}^2 J/M^2 \leq 1$ , and they can exhibit ergosurfaces, that consist of two parts, forming an ergo-Saturn.

The scalarization of rapidly rotating boson stars and hairy black holes allows their mass and particle number to exceed the maximal values allowed for their general relativistic counterparts. This effect seen here for the larger values of the rotational quantum number may be viewed as a downscaled version of what has been observed for neutron stars. It should be interesting to

increase the rotational quantum number further, to see how strong the effect of scalarization may become for rotating hairy black holes.

### Acknowledgment

We gratefully acknowledge support by the DFG within the Research Training Group 1620 "Models of Gravity" and by FP7, Marie Curie Actions, People, International Research Staff Exchange Scheme (IRSES-606096). We gratefully acknowledge discussions with E.Radu. J.K. gratefully acknowledges discussions with C.Lämmerzahl.

## References

- [1] P. Jordan, *Nature* **164** (1949) 637.
- [2] M. Fierz, *Helv. Phys. Acta* **29** (1956) 128.
- [3] P. Jordan, *Z. Phys.* **157** (1959) 112.
- [4] C. Brans and R. H. Dicke, *Phys. Rev.* **124** (1961) 925.
- [5] R. H. Dicke, *Phys. Rev.* **125** (1962) 2163.
- [6] T. Damour and G. Esposito-Farese, *Phys. Rev. Lett.* **70**, 2220 (1993).
- [7] D. D. Doneva, S. S. Yazadjiev, N. Stergioulas and K. D. Kokkotas, *Phys. Rev. D* **88**, no. 8, 084060 (2013).
- [8] D. D. Doneva, S. S. Yazadjiev, N. Stergioulas, K. D. Kokkotas and T. M. Athanasiadis, *Phys. Rev. D* **90**, no. 4, 044004 (2014).
- [9] A. W. Whinnett, *Phys. Rev. D* **61**, 124014 (2000).
- [10] M. Alcubierre, J. C. Degollado, D. Nunez, M. Ruiz and M. Salgado, *Phys. Rev. D* **81**, 124018 (2010).
- [11] M. Ruiz, J. C. Degollado, M. Alcubierre, D. Nunez and M. Salgado, *Phys. Rev. D* **86**, 104044 (2012).
- [12] H. Luckock and I. Moss, *Phys. Lett. B* **176**, 341 (1986).
- [13] M. S. Volkov and D. V. Galtsov, *JETP Lett.* **50**, 346 (1989) [*Pisma Zh. Eksp. Teor. Fiz.* **50**, 312 (1989)].
- [14] P. Breitenlohner, P. Forgacs and D. Maison, *Nucl. Phys. B* **383**, 357 (1992).
- [15] B. Kleihaus and J. Kunz, *Phys. Rev. D* **57**, 6138 (1998).
- [16] B. Kleihaus and J. Kunz, *Phys. Rev. Lett.* **86**, 3704 (2001).
- [17] B. Kleihaus, J. Kunz and F. Navarro-Lerida, *Phys. Lett. B* **599**, 294 (2004).
- [18] C. A. R. Herdeiro and E. Radu, *Phys. Rev. Lett.* **112**, 221101 (2014).
- [19] S. Hod, *Phys. Rev. D* **86**, 104026 (2012) [Erratum-*ibid.* *D* **86**, 129902 (2012)].
- [20] C. Herdeiro, E. Radu and H. Runarsson, *Phys. Lett. B* **739** (2014) 302.
- [21] C. Herdeiro and E. Radu, arXiv:1501.04319 [gr-qc].
- [22] W. Schönauer and R. Weiß, *J. Comput. Appl. Math.* **27**, 279 (1989) 279; M. Schauder, R. Weiß and W. Schönauer, The CADSOL Program Package, Universität Karlsruhe, Interner Bericht Nr. 46/92 (1992).

- [23] E. Berti, E. Barausse, V. Cardoso, L. Gualtieri, P. Pani, U. Sperhake, L. C. Stein and N. Wex *et al.*, arXiv:1501.07274 [gr-qc].